

Physical Constraints in Intracellular Signaling: The Cost of Sending a Bit

Samuel J. Bryant^{*}

Department of Physics, Yale University, New Haven, Connecticut 06511, USA

Benjamin B. Machta[†]

Department of Physics, Yale University and Quantitative Biology Institute, Yale University, New Haven, Connecticut 06511, USA

 (Received 18 July 2022; revised 20 March 2023; accepted 9 June 2023; published 7 August 2023)

Many biological processes require timely communication between molecular components. Cells employ diverse physical channels to this end, transmitting information through diffusion, electrical depolarization, and mechanical waves among other strategies. Here we bound the energetic cost of transmitting information through these physical channels, in $k_B T/\text{bit}$, as a function of the size of the sender and receiver, their spatial separation, and the communication latency. These calculations provide an estimate for the energy costs associated with information processing arising from the physical constraints of the cellular environment, which we find to be many orders of magnitude larger than unity in natural units. From these calculations, we construct a phase diagram indicating where each strategy is most efficient. Our results suggest that intracellular information transfer may constitute a substantial energetic cost. This provides a new tool for understanding tradeoffs in cellular network function.

DOI: [10.1103/PhysRevLett.131.068401](https://doi.org/10.1103/PhysRevLett.131.068401)

A large portion of energy consumption in biology goes toward information processing tasks. There have been many theoretical efforts to bound the energy needed for these tasks, including the cost of precisely reading DNA [1], performing abstract computation [2–7], measuring and sensing the environment [8–13], breaking time-reversal symmetry [14–18], keeping accurate time [19–21], self-replication [22], and controlling a small thermodynamic system [23–25]. The abstract nature of these bounds makes them broadly applicable, but often at the cost of divorcing them from the details of their physical implementations. For many cellular examples, the bounds appear dramatically far from saturated [26–29].

Biological systems are subject to constraints often not captured in these theoretical abstractions. In particular, information processing networks are by nature distributed in space and time. For example, chemoreceptors in bacteria measure environmental information that must then travel $\sim 1 \mu\text{m}$ from receptor clusters to cellular motors within a fraction of a second to be behaviorally useful. In neurons, information arriving at synapses in dendrites must travel across the cell body in timescales of milliseconds.

The schemes that have evolved to move information across space are varied, not just in their molecular details, but in their underlying physics. In neurons, signals are transmitted electrically via the opening of ion channels that depolarize the membrane, causing distant changes in electrical potential. All cells signal through the diffusion of second-messenger molecules. At the organism level,

pressure waves transmit information over longer distances in the form of sound.

While moving information is not a process that has a fundamental energetic cost, the practical costs can be substantial—a large fraction [30,31] of the energy humans consume is spent by neurons to generate voltage gradients, primarily used for sending signals [27].

In this Letter, we estimate bounds for this energetic cost of sending information. We examine several physical communication strategies used by biology: (1) electrical signaling via the depolarization of membranes through ion channels, (2) diffusive signaling in 2D and 3D, and (3) acoustic signaling. The resulting energetic costs, in $k_B T/\text{bit}$, depend on four key parameters: the distance the signal is sent r , the signal frequency ω , and the size of the sender and receiver σ_I and σ_O . The bounds we find do not represent fundamental costs associated with information processing, but instead represent costs associated with the constraints that biology faces, subject to life's existence in a watery buffer. As such our bounds contain not only pure numbers and $k_B T$, but also geometric factors, diffusion constants, membrane capacitances, and other parameters.

Like previous work, here we use thermodynamic tools to place energetic bounds on information processing at the cellular level. However, unlike previous analyses of information processing, here we focus on the cost of moving information, which we find to be shaped by the constraints imposed by the physical environments available to biology. The resulting costs we find are large and theoretically comprehensible, but can only be obtained by making

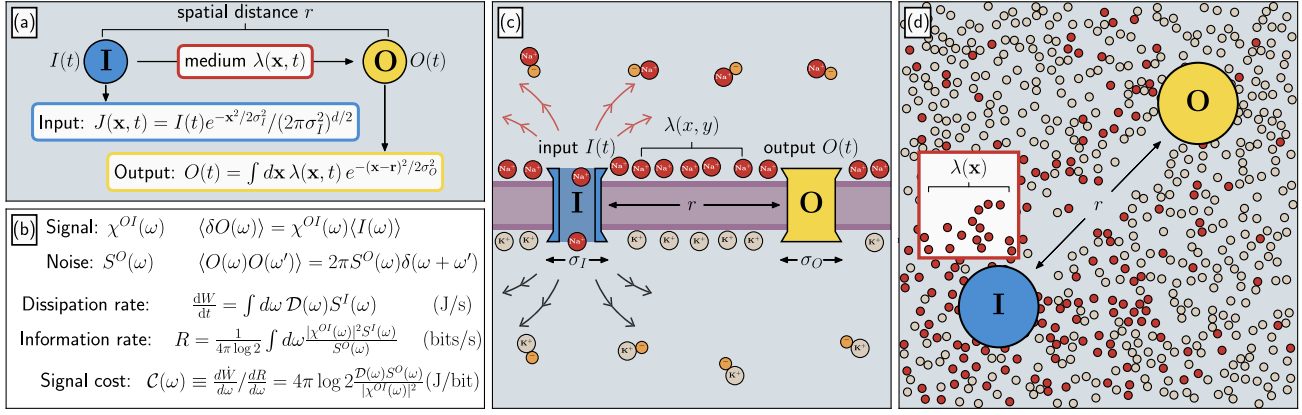


FIG. 1. An overview of spatial communication. (a) An abstract transmission scheme that sends information from a sender I to a receiver O . The sender locally modifies the density field λ with current density J , which propagates to the receiver where it is measured as a local perturbation $O(t)$. The input current density J is normalized to separate the effects of the input signal strength and its spatial distribution. The output O is not normalized, reflecting the fact that the receiver’s ability to resolve the signal increases with its size. (b) Outline of calculation for the energetic cost of communication, which depends on the signal transmission strength χ^{OI} , the thermal noise $S^O(\omega)$ in the output measurement, and the dissipation kernel $\mathcal{D}(\omega)$ of the input process. (c) Electrical communication between two ion channels in a membrane. The input signal $I(t)$ is the time-varying current flowing through the input ion channel. The output $O(t)$ is the excess charge accumulated at the output ion channel. The density field λ is the surface charge density on the membrane. (d) Diffusive signaling in 2D between two proteins embedded in a membrane.

reference to the physics of the system; they cannot be extracted from information-theoretic considerations alone.

Setup.—As summarized in Figs. 1(a) and 1(b), there is a sender I and a receiver O embedded in a background medium $\lambda(\mathbf{x}, t)$ subject to thermal fluctuations. The sender transmits a time-varying signal $I(t)$ by locally perturbing the medium λ . The receiver then measures the signal by observing $O(t)$, the local deviation of the medium λ from equilibrium. From this measurement, the receiver is able to extract information about the state of the sender. The input $I(t)$ is localized to a region of radius σ_I centered at the origin, and the output $O(t)$ is measured by a sensor a distance r away, of radius σ_O . We define these regions as Gaussian densities for mathematical simplicity. λ is a density field, whose nature and dynamics depend on the specific communication medium (see Table I).

We quantify the rate of information transfer between the sender and the receiver using the time-series mutual information rate between $I(t)$ and $O(t)$, measured in bits per second [45]. In our setup, this quantifies directed information transfer because the sender’s behavior is externally specified, with no feedback from the output, obviating the need for measures like the transfer entropy [46–48]. Following [45], we assume that we are in the weak signal regime and further that noise is dominated by thermal fluctuations in λ . With this assumption, the rate that information is sent from the input to the output is

$$R(I, O) \approx \frac{1}{4\pi \log 2} \int d\omega \frac{|\chi^{OI}(\omega)|^2 S^I(\omega)}{S^O(\omega)} \quad (\text{bits/s}), \quad (1)$$

where $|\chi^{OI}|^2$ and $S^O(\omega)$ correspond to the transmission gain and noise, as defined in Fig. 1(b), and where $S^I(\omega)$ is the power spectrum of the signal process, chosen by the sender, and thus external to the network itself.

To compute the energetic cost of signaling, we need to compare the information rate to the rate of work required to produce the input signal. We characterize this dissipation rate \dot{W} by a dissipation kernel function $\mathcal{D}(\omega)$, describing the rate of energy dissipation at each signal frequency [Fig. 1(b)]. The overall cost per bit at frequency ω is the ratio of the dissipation rate integrand to the information rate integrand (see Supplemental Material [32]),

$$\mathcal{C}(\omega) \equiv \frac{\text{cost}}{\text{bit}} \equiv \frac{d\dot{W}}{d\omega} / \frac{dR}{d\omega} = 4\pi \log 2 \frac{\mathcal{D}(\omega) S^O(\omega)}{|\chi^{OI}(\omega)|^2}. \quad (2)$$

Characterizing this for a given model requires computing the equilibrium noise spectrum $S^O(\omega)$, the dissipation kernel $\mathcal{D}(\omega)$, and the transmission coefficient $\chi^{OI}(\omega)$. We sketch this analysis explicitly for the case of electrical signaling in membranes. The detailed analysis for this and the other systems (diffusive and acoustic signaling) is found in the Supplemental Material [32].

Electrical communication.—We suppose there is a signaling process between two ion channels bound to a 2D membrane embedded in a bulk 3D environment extending in the z direction [Fig. 1(c)]. Current may flow through the bulk via the movement of charged ions, which we model as a resistive material obeying Laplace’s equation ($\nabla^2 V = 0$) with conductance α (Ω^{-1}/m) (Supplemental Material Sec. 3.6 [32]). Free charges may accumulate at the

TABLE I. A summary of the setup and energetic cost of sending information for four classes of physical communication systems. Each system has a coupling field λ , which transmits the signal with dynamics specific to that system. The sender couples to λ via $\partial_t \lambda = (\partial_t \lambda)_0 + J(x, t)$. \mathcal{C} is the computed energetic cost to send information in units of $k_B T/\text{bit}$ when the transmission distance r is smaller than the system-specific characteristic length scale ℓ . Derivations and explanations of these models can be found in the Supplemental Material [32].

System, example	Coupling field λ , dynamics	Input $I(t)$, output $O(t)$	Energy cost \mathcal{C}	Length scale
Electrical, ion channels in neurons	Surface charge density (C/m ²) $\partial_t \lambda(\mathbf{k}, t) = -(\alpha k/c)\lambda(\mathbf{k}, t)$	$I(t) = \text{injected current (A)}$ $O(t) = \text{excess charge (C)}$	$\mathcal{C}^{\text{EI}} = \pi \log 2 (r^2/\sigma_I \sigma_O)$	$\ell(\omega) = (\alpha/\omega c)$
Diffusion 2D, Pip2	Messenger density (1/m ²) $\partial_t \lambda(\mathbf{x}, t) = D \nabla^2 \lambda(\mathbf{x}, t)$	$I(t) = \text{activation rate (Hz)}$ $O(t) = \text{messenger count (1)}$	$\mathcal{C}^{\text{D2}} \approx 4 \log 2 \{ \log(\ell/\sigma_I) \log(\ell/\sigma_O) / \log[(\ell/r)^2] \}$	$\ell(\omega) = \sqrt{(D/\omega)}$
Diffusion 3D, CheY in <i>E. coli</i>	Messenger density (1/m ³) $\partial_t \lambda(\mathbf{x}, t) = D \nabla^2 \lambda(\mathbf{x}, t)$	$I(t) = \text{activation rate (Hz)}$ $O(t) = \text{messenger count (1)}$	$\mathcal{C}^{\text{D3}} = (4 \log 2/\pi)(r^2/\sigma_I \sigma_O)$	$\ell(\omega) = \sqrt{(D/\omega)}$
Acoustic, Speech	Medium density (kg/m ³) $\partial_t^2 \lambda - c^2 (\tau \partial_t)^n \nabla^2 \lambda = c^2 \nabla^2 \lambda$	$I(t) = \text{injected mass (kg/s)}$ $O(t) = \text{excess density (kg)}$	$\mathcal{C}^{\text{Ac}} = (2 \log 2/\pi)(r^2 \ell_\sigma^2/\sigma_I \sigma_O^3)$	$\nu = (i\tau\omega)^\eta$ $\ell = (c/\omega)/\text{Im}(\nu)$ $\ell_\sigma = (c/\omega)\text{Im}(\nu)$

membrane, which we treat as having uniform capacitance c (F/m²). The surface charge density at the membrane is given by $\lambda(x, y)$.

Following Fig. 1(a), the input of the system $I(t)$ is the time-varying flow of current through the sender ion channel located at the origin. The output of the system $O(t)$ is the excess charge at the receiver. We assume an infinite flat membrane, though the geometry of specific systems is likely important.

Linearized dynamics.—To compute (2), we need a minimal model for the dynamics of λ . At the membrane, the voltage is given by the local capacitance equation: $V(x, y) = \lambda(x, y)/c - h(x, y)$, where h is an artificial external field useful in calculating the spectrum of thermal charge fluctuations. Bulk current flows according to $-\alpha \nabla V$, which is divergenceless everywhere except at the membrane. Thus, the rate of change of charge at the membrane is given by the sum of the injected current $J(x, y)$ and the rate that charge accumulates from bulk currents: $\partial_t \lambda(x, y) = J(x, y) + \alpha \partial_z V(x, y, z)|_{z=0}$. These equations are linear, and in xy -Fourier space they close in terms of λ and applied fields h and J yielding

$$\partial_t \lambda(\mathbf{k}, t) = -\alpha k \left[\frac{\lambda(\mathbf{k}, t)}{c} - h(\mathbf{k}, t) \right] + J(\mathbf{k}, t), \quad (3)$$

where \mathbf{k} is the xy -momentum vector (all Fourier transforms are implicit).

Calculating transmission strength χ^{OI} .—The transmission strength is characterized by the linear response function χ^{OI} which indicates how the mean output $\langle O(t) \rangle$

responds to the input $I(t)$. We first compute the response of the charge density to the input signal $\chi^{\lambda J}$ in frequency space by reading off the frequency-space Fourier transform of Eq. (3): $\chi^{\lambda J}(k, \omega) = c/\alpha(|k| + i\omega c/\alpha)$. By then integrating $\chi^{\lambda J}$ over the sensor area, we get the transmission coefficient χ^{OI} ,

$$|\chi^{OI}(\omega)|^2 = \frac{c^2 \sigma_O^4}{\alpha^2 r^2} U_S \left(\frac{r}{\ell(\omega)} \right), \quad \ell(\omega) = \frac{\alpha}{\omega c}, \quad (4)$$

where U_S is a universal function of its argument that goes to 1 when $r/\ell(\omega) \ll 1$ and then quickly decays (see Supplemental Material Sec. 3 [32]). Importantly, we have expressed this universal function in terms of the length scale $\ell(\omega) = \alpha/\omega c$, which sets an upper limit on the viability of transmission. The origin of this length scale is related to the RC timescale found in basic RC circuits. The 3D bulk resistance and 2D membrane capacitance together define an RC (inverse) *velocity*, or equivalently, a length scale at a given frequency.

Calculating dissipation $\mathcal{D}(\omega)$.—In the linear response regime, the instantaneous dissipation associated with powering a transmembrane current is given by a spatial integral of the injected current density multiplied by the voltage across the membrane. In frequency space, this can be calculated from the response function, yielding

$$\mathcal{D}(\omega) = \frac{1}{8\pi^{3/2} \alpha \sigma_I} U_D \left(\frac{\sigma_I}{\ell(\omega)} \right), \quad (5)$$

where $U_D(\sigma/\ell \ll 1) \sim 1$ is another universal function.

Calculating noise S^O .—We define the noise $S^O(\omega)$ to be the power spectrum of the equilibrium fluctuations in the output $O(t)$ in the absence of an input signal. As with χ^{OI} , we first compute $\chi^{\lambda h}$, the susceptibility of the charge density field to the external field h , by reading off Eq. (3): $\chi^{\lambda h}(\mathbf{k}, \omega) = \alpha k / (\alpha k / c + i\omega)$. The fluctuation dissipation theorem [49] then tells us that the equilibrium fluctuations of λ are related to the imaginary part of $\chi^{\lambda h}$: $S^\lambda(\omega) = -(2k_B T / \omega) \text{Im}(\chi^{\lambda h})$. We integrate S^λ over the sensor area to obtain $S^O(\omega)$,

$$S^O = \frac{2\pi^{3/2} k_B T c^2 \sigma_O^3}{\alpha} U_N \left(\frac{\sigma_O}{\ell(\omega)} \right), \quad (6)$$

where, again, $U_N(\sigma_O / \ell \ll 1) \sim 1$ is a universal function.

Energetic cost per bit.—Plugging these results into Eq. (2) yields the energetic cost of sending an electric signal at frequency ω over a distance r between two ion channels,

$$\mathcal{C}^{\text{El}} = \pi \log 2 \frac{r^2}{\sigma_I \sigma_O} U^{\text{El}} \left(\frac{r}{\ell(\omega)} \right) \quad (k_B T / \text{bit}). \quad (7)$$

We refer to $\pi \log 2 r^2 / \sigma_I \sigma_O$ as the “scaling” cost and to U^{El} as the length scale correction, which can be ignored when the transmission distance r is smaller than the characteristic length scale $\ell(\omega)$. When $r \ll \ell(\omega)$, the cost per bit is independent of the system constants and frequency; it depends only on the length scales r , σ_I , σ_O . However, when $r \gg \ell(\omega)$, the correction function U^{El} blows up, and the cost becomes large [Fig. 2(c), lower panel].

Comparing strategies.—In addition to electrical signaling, we also considered the energetic cost of sending

information via diffusive signaling in 2D and 3D and acoustic signaling. The setup and results are summarized in Table I, with detailed derivations provided in the Supplemental Material [32]. Figure 2(a) shows the resulting phase diagram with respect to frequency and distance, indicating where each method of signaling is energetically preferred. For all of these systems, the cost of signaling diverges as the sensor size goes to zero, reflecting the fact that an infinitesimal sender has an infinite resistance and an infinitesimal receiver cannot resolve a signal.

Each of these systems has a characteristic length scale $\ell(\omega)$, which determines its limits of viability [Fig. 2(b)], given in Table I. When the transmission distance exceeds this length scale, the energetic cost of sending information no longer follows the scaling forms \mathcal{C} , instead becoming exponentially expensive. Below their characteristic length scales, the cost of communication for 3D diffusion, electrical and acoustic signaling scale with r^2 . Therefore, the transition lines between the phases in Fig. 2(a) can be determined by their characteristic length scales, which set the cutoff in energetic efficiency. Diffusive signaling in 2D has a unique scaling form and is preferred over 3D diffusive signaling, except in the regime where diffusion in 2D would be too slow; typical membrane diffusion constants are 2–3 orders of magnitude slower than those for small molecules in the cytoplasm.

For diffusive and electrical signaling, the frequency ω can be interpreted as measuring the speed of signal transmission. These two physical mediums do not support coherent waves and so a signal must reach the receiver before it phase shifts and is strongly attenuated. In diffusive signaling in d dimensions, for example, this means that the transmission distance is limited to the half-period diffusive

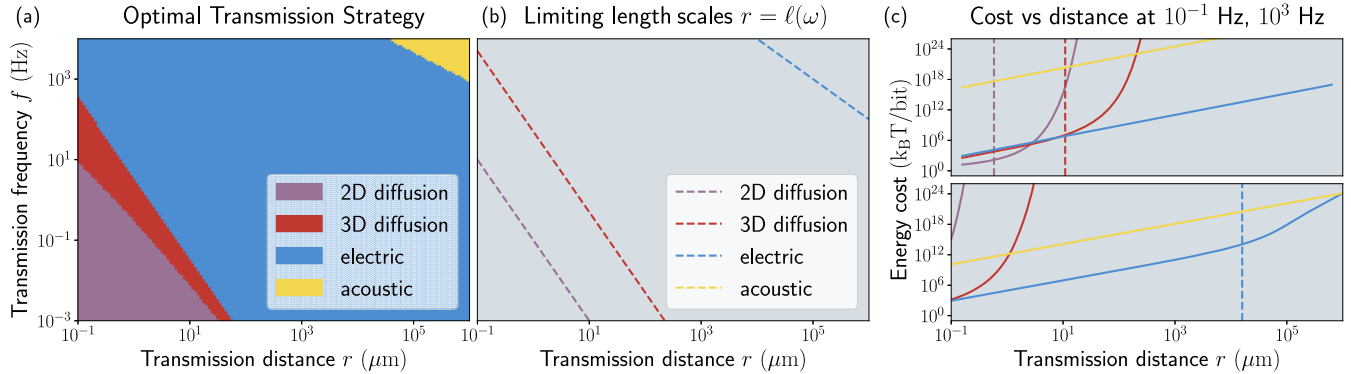


FIG. 2. An illustration of the energetic cost of communication for four signaling mechanisms: 2D diffusive signaling (purple), 3D diffusive signaling (red), electrical-membrane signaling (blue), and acoustic signaling in saline water (yellow). Here, the sender-receiver sizes are fixed at $\sigma_I = \sigma_O = 5$ nm. Diffusion: $D = 0.1 \mu\text{m}^2/\text{s}$ ($d = 2$), $D = 50 \mu\text{m}^2/\text{s}$ ($d = 3$), typical values in the plasma membrane and cytoplasm [50]. Electrical: $\alpha = 10^{-6} \text{ S}/\mu\text{m}$ [51], $c = 10^{-14} \text{ F}/\mu\text{m}^2$ [52]. Acoustic: $c = 1.5 \times 10^9 \mu\text{m}/\text{s}$, $\eta = 0.21$, $\tau^\eta = 8.9 \times 10^{-5} (s^\eta)$ (extracted from ultrasound measurements in blood, see Supplemental Material Sec. 5.2 [32]). (a) The optimality phase space. For each value of signal distance and frequency, the color of the optimal signaling mechanism is displayed. (b) The characteristic length scale ℓ is plotted for each signaling mechanism. These draw exclusion zones dictating where signaling mechanisms become prohibitively expensive. (c) The energetic cost of sending information is plotted for each signaling mechanism as a function of distance at a transmission frequency of 0.1 Hz (top) and 1 kHz (bottom).

travel distance $r^2 < \langle \Delta x^2 \rangle = 2d\pi D/\omega$, explaining the appearance of the length scale $\ell(\omega) = \sqrt{D/\omega}$.

Acoustic signaling is different in that it permits coherent waves which move at speed c . For these waves, the damping coefficient τ sets two characteristic scales. The inverse attenuation ℓ sets the length over which a plane wave is attenuated and thus the cutoff for the scaling regime. In addition, l_σ sets the length below which pressure fluctuations are overdamped and do not propagate as waves, around $10\ \mu\text{m}$ in the cellular environment [53], much larger than subcellular sensors. For sensors smaller than this second length scale, noise is dominated by these slower decaying, nonpropagating modes. In this regime, we find acoustic signaling is less efficient than electrical signaling by a factor of $(l_\sigma/\sigma_O)^2 \sim 10^6$ (Supplemental Material Sec. 5 [32]). This provides a possible energetic explanation for why acoustic signaling is absent at the cellular level despite its ubiquity in larger organisms.

Outlook.—The energetic costs we have obtained are lower bounds that hold regardless of the molecular mechanism being used to power the communication channel, which can be quite varied. For example, diffusive signaling can be driven by reaction cycles (e.g., in CheY phosphorylation-dephosphorylation cycles which in net hydrolyze ATP) or by chemical pumps that concentrate signal molecules for controlled release (e.g., neurotransmitter concentration in synaptic vesicles). For each of these processes, the total dissipation required to power the channel may be larger than the bounds we derive, but cannot be smaller. The bounds also apply regardless of how the information is ultimately read out. The continuous output signal used here may be needed in other forms, such as the binary switching state of a flagellar motor. Such lossy signal conversions involve a reduction of information and are thus still bounded by our results [54].

There are some limitations in this analysis. Our results often assume a simplified geometry. In electrical signaling, axons and dendrites are roughly cylindrical, rather than the 2D sheets used here, qualitatively changing results when signals are sent a distance farther than the cylinder radius. And in a membrane enclosed region, diffusive signals do not potentiate indefinitely, changing the form of our bound when the diffusive length scale becomes larger than the length of the region. Our bounds are approximate in that we make use of linearized equations for the media, which is a good model for these systems in biological contexts. In this approximation, driving further from equilibrium decreases information efficiency. The small nonlinearities in these systems could make small changes to our approximate bounds in either direction. Our setup also does not capture some physical strategies, such as the manipulation of stresses in fiber networks and directed transport by motor proteins. The noise in this calculation is assumed to be thermal noise arising from equilibrium fluctuations. There may also be other design principles that are not covered by

our bounds. We do not consider the cost of building and maintaining the protein machinery required to run these communication channels. For sending information over longer ranges, biology often uses relays, where information is sent through an excitable medium, often as an energy consuming traveling wave, a mechanism of information transfer not discussed in this Letter.

Prior work that investigates the cost of computation often considers either the Landauer limit [2,8,12,55] required to erase information or the cost of breaking time-reversal symmetry [14,15,19–21,25]. While these results are fundamental, they produce bounds on the order of $k_B T$, far below the energetic scale seen in real processes. In contrast, the results obtained here depend on physical constants as well as practical constraints like the size of the sensors and the transmission distance, producing energetic constraints orders of magnitude larger. For example, for a diffusive signal sent in 3D over a distance $r \sim 1\ \mu\text{m}$, with sensor sizes on the order of $\sigma \sim 10\ \text{nm}$, the cost is on the order of $10^4 k_B T$. Thus the large costs that biology must pay to process information *can* be understood theoretically, albeit only by additionally considering the physical constraints on real biological systems. In conjunction with a range of recent efforts to quantify information transfer across biological scales [48,56–58], we hope that follow-ups to this Letter will be able to quantify a computational budget required for these processes, which in many cases appears to be substantial [26,28].

We thank Isabella Graf, Henry Mattingly, and Mason Rouches for useful comments on the manuscript, as well as Sverre Holm for discussions on acoustic phenomena, and especially James Sethna for inspiring discussions. The work was funded by NIH R35 GM138341, NSF 1808551, and a Simons Investigator grant.

*samuel.bryant@yale.edu

†benjamin.machta@yale.edu

- [1] J. J. Hopfield, *Proc. Natl. Acad. Sci. U.S.A.* **71**, 4135 (1974).
- [2] R. Landauer, *IBM J. Res. Dev.* **5**, 183 (1961).
- [3] C. H. Bennett, *Int. J. Theor. Phys.* **21**, 905 (1982).
- [4] D. H. Wolpert, *J. Phys. A* **52**, 193001 (2019).
- [5] H.-L. Chen, D. Doty, and D. Soloveichik, [arXiv:1204.4176](https://arxiv.org/abs/1204.4176).
- [6] A. W. Eckford, B. Kuznets-Speck, M. Hinczewski, and P. J. Thomas, in *2018 IEEE International Symposium on Information Theory (ISIT)* (IEEE,vail CO, 2018), pp. 2545–2549, ISSN: 2157-8117.
- [7] A. Kolchinsky and D. H. Wolpert, *Phys. Rev. E* **104**, 034129 (2021).
- [8] P. Mehta and D. J. Schwab, *Proc. Natl. Acad. Sci. U.S.A.* **109**, 17978 (2012).
- [9] C. C. Govern and P. R. ten Wolde, *Phys. Rev. Lett.* **113**, 258102 (2014).
- [10] T.-L. Wang, B. Kuznets-Speck, J. Broderick, and M. Hinczewski, The price of a bit: energetic costs and the

- evolution of cellular signaling (2020), [10.1101/2020.10.06.327700](https://doi.org/10.1101/2020.10.06.327700).
- [11] T. E. Ouldridge, C. C. Govern, and P. R. ten Wolde, *Phys. Rev. X* **7**, 021004 (2017).
- [12] P. Sartori, L. Granger, C. F. Lee, and J. M. Horowitz, *PLoS Comput. Biol.* **10**, e1003974 (2014).
- [13] A. C. Barato, D. Hartich, and U. Seifert, *Phys. Rev. E* **87**, 042104 (2013).
- [14] E. H. Feng and G. E. Crooks, *Phys. Rev. Lett.* **101**, 090602 (2008).
- [15] J. M. R. Parrondo, C. V. d. Broeck, and R. Kawai, *New J. Phys.* **11**, 073008 (2009).
- [16] A. C. Barato and U. Seifert, *Phys. Rev. Lett.* **114**, 158101 (2015).
- [17] A. I. Brown and D. A. Sivak, *Phys. Rev. E* **94**, 032137 (2016).
- [18] R. Rao and M. Esposito, *Phys. Rev. X* **6**, 041064 (2016).
- [19] Y. Cao, H. Wang, Q. Ouyang, and Y. Tu, *Nat. Phys.* **11**, 772 (2015).
- [20] A. C. Barato and U. Seifert, *Phys. Rev. X* **6**, 041053 (2016).
- [21] D. Zhang, Y. Cao, Q. Ouyang, and Y. Tu, *Nat. Phys.* **16**, 95 (2020).
- [22] J. L. England, *J. Chem. Phys.* **139**, 121923 (2013).
- [23] D. A. Sivak and G. E. Crooks, *Phys. Rev. Lett.* **108**, 190602 (2012).
- [24] B. B. Machta, *Phys. Rev. Lett.* **115**, 260603 (2015).
- [25] S. J. Bryant and B. B. Machta, *Proc. Natl. Acad. Sci. U.S.A.* **117**, 3478 (2020).
- [26] J. Rodenfels, K. M. Neugebauer, and J. Howard, *Dev. Cell* **48**, 646 (2019).
- [27] W. B. Levy and V. G. Calvert, *Proc. Natl. Acad. Sci. U.S.A.* **118**, e2008173118 (2021).
- [28] D. Attwell and S. B. Laughlin, *J. Cereb. Blood Flow Metab.* **21**, 1133 (2001).
- [29] S. B. Laughlin, R. R. de Ruyter van Steveninck, and J. C. Anderson, *Nat. Neurosci.* **1**, 36 (1998).
- [30] A. J. Smith, H. Blumenfeld, K. L. Behar, D. L. Rothman, R. G. Shulman, and F. Hyder, *Proc. Natl. Acad. Sci. U.S.A.* **99**, 10765 (2002).
- [31] M. E. Raichle and D. A. Gusnard, *Proc. Natl. Acad. Sci. U.S.A.* **99**, 10237 (2002).
- [32] See Supplemental Material at <http://link.aps.org/supplemental/10.1103/PhysRevLett.131.068401> for the full analysis, which includes Refs. [33–44].
- [33] F. W. J. Olver and National Institute of Standards and Technology (U.S.), *NIST Handbook of Mathematical Functions* (Cambridge University Press: NIST, Cambridge, New York, 2010).
- [34] A.-F. Bitbol and N. S. Wingreen, *Biophys. J.* **108**, 1293 (2015).
- [35] M. G. Wismer, *J. Acoust. Soc. Am.* **120**, 3493 (2006).
- [36] S. Holm and R. Sinkus, *J. Acoust. Soc. Am.* **127**, 542 (2010).
- [37] M. J. Holmes, N. G. Parker, and M. J. W. Povey, *J. Phys. Conf. Ser.* **269**, 012011 (2011).
- [38] J. Lin, C. Scalo, and L. Hesselink, [arXiv:1707.05876](https://arxiv.org/abs/1707.05876).
- [39] A. S. Dukhin and P. J. Goetz, *J. Chem. Phys.* **130**, 124519 (2009).
- [40] H. E. Bass, L. C. Sutherland, and A. J. Zuckerwar, *J. Acoust. Soc. Am.* **88**, 2019 (1990).
- [41] P. M. Morse and K. U. Ingard, *Theoretical Acoustics* (McGraw-Hill, New York, 1968).
- [42] M. A. Ainslie and J. G. McColm, *J. Acoust. Soc. Am.* **103**, 1671 (1998).
- [43] F. A. Duck, in *Physical Properties of Tissues* (Academic Press, London, 1990).
- [44] W. Bialek, *Biophysics: Searching for Principles* (Princeton University Press, Princeton, 2012).
- [45] F. Tostevin and P. Rein ten Wolde, *Phys. Rev. Lett.* **102**, 218101 (2009).
- [46] T. Schreiber, *Phys. Rev. Lett.* **85**, 461 (2000).
- [47] S. Lahiri, P. Nghe, S. J. Tans, M. L. Rosinberg, and D. Lacoste, *PLoS One* **12**, 1 (2017).
- [48] H. H. Mattingly, K. Kamino, B. B. Machta, and T. Emonet, *Nat. Phys.* **17**, 1426 (2021).
- [49] R. Zwanzig, *Nonequilibrium Statistical Mechanics* (Oxford University Press, Oxford, New York, 2001).
- [50] P. E. Schavemaker, A. J. Boersma, and B. Poolman, *Front. Mol. Biosci.* **5**, 93 (2018).
- [51] K. Wang, J. Riera, H. Enjieu-Kadji, and R. Kawashima, *Neural Comput.* **25**, 1807 (2013).
- [52] L. J. Gentet, G. J. Stuart, and J. D. Clements, *Biophys. J.* **79**, 314 (2000).
- [53] S. Holm, *Waves with Power-Law Attenuation* (Springer International Publishing, Cham, 2019).
- [54] T. M. Cover and J. A. Thomas, *Elements of Information Theory 2nd Edition*, Wiley Series in Telecommunications and Signal Processing (Wiley-Interscience, New York, 2006).
- [55] J. Fuchs, S. Goldt, and U. Seifert, *Europhys. Lett.* **113**, 60009 (2016).
- [56] I. Nemenman, W. Bialek, and R. de Ruyter van Steveninck, *Phys. Rev. E* **69**, 056111 (2004).
- [57] T. Gregor, D. W. Tank, E. F. Wieschaus, and W. Bialek, *Cell* **130**, 153 (2007).
- [58] I. R. Graf and B. B. Machta, [arXiv:2305.05647](https://arxiv.org/abs/2305.05647).